

# Squeezing evolution with non-dissipative $SU(1, 1)$ systems

Faisal A. A. El-Orany,<sup>1,\*</sup> S. S. Hassan,<sup>2,†</sup> and M. Sebawe Abdalla<sup>3</sup>

<sup>1</sup>*Department of Mathematics and computer Science,*

*Faculty of Science, Suez Canal University 41522, Ismailia, Egypt;*

<sup>2</sup>*University of Bahrain, College of Science,*

*Mathematics Department, P.O. Box 32038, Bahrain*

<sup>3</sup>*Mathematics Department, College of Science,*

*King Saud University, P.O. Box 2455, Riyadh 11451, Saudi Arabia*

(Dated: December 9, 2018)

We investigate the squeezed regions in the phase plane for non-dissipative dynamical systems controlled by  $SU(1, 1)$  Lie algebra. We analyze such study for the two  $SU(1, 1)$  generalized coherent states, namely, the Perelomov coherent state (PCS) and the Barut-Girardello Coherent state (BGCS).

PACS numbers: 42.50.Dv, 42.50.-p

## I. INTRODUCTION

The  $SU(1, 1)$  algebra (together with the  $SU(2)$  algebra) has been much utilised in the theoretical study of the non-classical aspects of light in various quantum optical systems. For example: (i) The single-mode and the two-mode squeezed vacuum states of light, each with different bosonic algebraic realisation, are Perelomov-type  $SU(1, 1)$  coherent states [1]. (ii) The even and odd coherent states of light [2, 3] are one-mode bosonic realisation of the  $SU(1, 1)$  Lie algebra. (iii) The generalized Barut-Girardello coherent state is two-mode bosonic algebraic realisation of the  $SU(1, 1)$  Lie algebra [4]: such states were used in the theoretical description of coherent pion production in high energy collision processes (see [5] and references therein) and within the framework of field theory in connection with "charged coherent state" representation for an Abelian charged massless boson field in the one-dimensional [6] and infinitely many degrees of freedom [7] cases. Within the context of the field of quantum optics, Agarwal [8] introduced the name "pair coherent states" to such generalised coherent states. (iv) The  $SU(1, 1)$  Lie algebra appears as the dynamical group of the quantum harmonic oscillator (, e.g. [9]). On the experimental side, optical interferometers

---

\*Electronic address: el'orany@hotmail.com; faisal.orany@mimos.my

†Electronic address: Shoukryhassan@hotmail.com

like four-wave mixers [10, 11] are characterised by  $SU(1,1)$  Lie algebra (for different schemes of generating the  $SU(1,1)$  states see [12, 13] and references therein). Study of squeezing properties associated with the  $SU(1,1)$  (as well  $SU(2)$ ) states aims mainly at the reduction of the quantum noise in the act of measurements in fields like spectroscopy [14] and interferometry [15].

In the present paper we study the time evolution of the squeezed regions associated with a non-dissipative model Hamiltonian which is presented as the linear combination of the generators of the  $SU(1,1)$  Lie algebra. For initial conditions, we consider the two  $SU(1,1)$  generalised coherent states, namely, the Perelomov coherent state (PCS) and the Barut-Girardello Coherent state (BGCS). The present study complements similar investigation for the  $SU(2)$  Lie algebraic representation state [16]. Nevertheless, it is worth referring to [17] in which  $SU(1,1)$  squeezing has been analysed for the  $SU(1,1)$  generalised coherent states when they are evolving in the nonabsorbing nonlinear media modelled as anharmonic oscillator. The dynamics related to such system is simpler than that in the present paper, as we shall see in the following section. Further in [17] the author shows for the initial  $SU(1,1)$  squeezed states (, e.g. the PCS) that the system can destroy the initial squeezing as well as can generate squeezing in the unsqueezed quadrature much greater than that in the initial squeezed conjugate quadrature. Also for the initial  $SU(1,1)$  unsqueezed states (, e.g. the BGCS) maximum squeezing can be observed *only* when the initial intensity of the field is very large.

The paper is organized in the following sequences: In section 2 we give the model Hamiltonian, the solution of the associated Heisenberg equations of motion and the basic relations and equations which will be used in the paper. In sections 3 and 4 we discuss the evolution of the squeezed regions for the PCS and BGCS state, respectively. The results are summarized in section 5.

## II. MODEL HAMILTONIAN AND OPERATOR SOLUTIONS

In this section we give the basic relations and equations, which will be mainly used throughout the paper. The relations include the model Hamiltonian and its associated operators solutions, the definitions of both the Perelomov  $SU(1,1)$  coherent state (PCS) [1], the Barut-Girardello coherent state (BGCS) [4] and  $SU(1,1)$  squeezing.

Now we consider a non-dissipative Hamiltonian model of the form (in units of  $\hbar = 1$ ),

$$\hat{H} = 2\omega\hat{k}_z + \lambda(\hat{k}_+ + \hat{k}_-), \quad (1)$$

where  $\hat{k}_z$  is a hermitian operator,  $\hat{k}_+ = (\hat{k}_-)^{\dagger}$  are raising (lowering) operators,  $\lambda$  is a suitable

coupling parameter and  $\omega$  is a frequency specifying the model. For the  $SU(1,1)$  Lie algebra the operators  $\hat{k}_{\pm,z}$  satisfy the following commutators:

$$[\hat{k}_+, \hat{k}_-] = -2\hat{k}_z, \quad [\hat{k}_z, \hat{k}_{\pm}] = \pm\hat{k}_{\pm}. \quad (2)$$

Note the Hamiltonian (1) represents either a degenerate or non-degenerate parametric amplifier (, e.g. [18]) according to the single mode boson representation  $\hat{k}_z = \frac{1}{2}(\hat{a}^\dagger\hat{a} + \frac{1}{2})$ ,  $\hat{k}_+ = \frac{1}{2}\hat{a}^{\dagger 2}$  or the two-mode boson representation  $\hat{k}_z = \frac{1}{2}(\hat{a}^\dagger\hat{a} + \hat{b}^\dagger\hat{b} + 1)$ ,  $\hat{k}_+ = \hat{a}^\dagger\hat{b}^\dagger$ , respectively. In both cases the operators  $\hat{k}_z, \hat{k}_{\pm}$  obey the  $SU(1,1)$  Lie algebra in (2). For convenience we define the following operators:

$$\hat{k}_x = \frac{1}{2}(\hat{k}_+ + \hat{k}_-), \quad \hat{k}_y = \frac{1}{2i}(\hat{k}_+ - \hat{k}_-), \quad (3)$$

where the set  $\{\hat{k}_x, \hat{k}_y, \hat{k}_z\}$  satisfies the following commutation rules

$$[\hat{k}_x, \hat{k}_y] = -i\hat{k}_z, \quad [\hat{k}_y, \hat{k}_z] = i\hat{k}_x, \quad [\hat{k}_z, \hat{k}_x] = i\hat{k}_y. \quad (4)$$

The associated Heisenberg uncertainty relation regarding the first commutator in (4) takes the form

$$\langle(\Delta\hat{k}_x)^2\rangle\langle(\Delta\hat{k}_y)^2\rangle \geq \frac{1}{4}|\langle\hat{k}_z\rangle|^2, \quad (5)$$

where  $\langle(\Delta\hat{k}_j)^2\rangle = \langle\hat{k}_j^2\rangle - \langle\hat{k}_j\rangle^2$ . To measure squeezing, we define the functions

$$F_j = \frac{\langle(\Delta\hat{k}_j)^2\rangle - \frac{1}{2}|\langle\hat{k}_z\rangle|}{\frac{1}{2}|\langle\hat{k}_z\rangle|}, \quad j = x, y. \quad (6)$$

Squeezing (reduction) in the fluctuation of the  $\hat{k}_x$ - or  $\hat{k}_y$ -components occurs if  $F_x < 1$  or  $F_y < 1$ , respectively, and maximum squeezing is reached when  $F_x = -1$  or  $F_y = -1$ .

Now, the evolution of the operators  $\{\hat{k}_x, \hat{k}_y, \hat{k}_z\}$  according to the Hamiltonian (1) and the relations (3), (4) are obtained by solving the corresponding Heisenberg equations of motion, which read [16, 19]

$$\begin{aligned} \hat{k}_x(t) &= R_1(t)\hat{k}_x(0) - J(t)\hat{k}_y(0) - S(t)\hat{k}_z(0) \\ \hat{k}_y(t) &= J(t)\hat{k}_x(0) + R_2(t)\hat{k}_y(0) + V(t)\hat{k}_z(0) \\ \hat{k}_z(t) &= S(t)\hat{k}_x(0) + V(t)\hat{k}_y(0) + R_3(t)\hat{k}_z(0), \end{aligned} \quad (7)$$

where the  $c$ -number time-dependent coefficients have the forms

$$\begin{aligned} R_1(t) &= \cos(2gt) - \frac{2\lambda^2}{g^2} \sin^2(gt), & R_2(t) &= \cos(2gt), \\ R_3(t) &= \cos(2gt) + \frac{2\omega^2}{g^2} \sin^2(gt), & J(t) &= \frac{\omega}{g} \sin(2gt), \\ S(t) &= \frac{2\omega\lambda}{g^2} \sin^2(gt), & V(t) &= \frac{\lambda}{g} \sin(2gt), \end{aligned} \quad (8)$$

and  $g = \sqrt{\omega^2 - \lambda^2}$ . It is clear that when  $\omega > \lambda$  the coefficients in (7) are periodic in the scaled time ( $gt$ ) with period  $2\pi$ .

For convenience we give some remarks on the Hamiltonian of the nonabsorbing nonlinear media, which can be modelled as anharmonic oscillator. This Hamiltonian—in the framework of  $SU(1, 1)$  Lie algebra generators—takes the form [17]:

$$\hat{H} = \omega \hat{k}_z + \lambda \hat{k}_+ \hat{k}_-, \quad (9)$$

where the notations have the same meaning as given above. In the bosonic language (9) represents the Kerr media Hamiltonian. For (9) one can easily show that  $\hat{k}_z$  and  $\hat{k}_+ \hat{k}_-$  are constants of motion, and the solutions of Heisenberg equations are

$$\hat{k}_z(t) = \hat{k}_z(0), \quad \hat{k}_+(t) = \hat{k}_+(0) \exp[it(\omega + 2\lambda \hat{k}_z)]. \quad (10)$$

It is obvious that the interaction Hamiltonian (9) provides an overall phase factor in the evolution operators  $\hat{k}_\pm(t)$ , i.e. it preserves the photon statistics of the system. Keeping this in mind and comparing (7) and (10) one can conclude that the dynamics associated with (9) is so simple compared to that of (1).

We proceed by considering two types of  $SU(1, 1)$  states, namely, the Perelomov  $SU(1, 1)$  coherent state (PCS) [1] and the Barut-Girardello coherent state (BGCS) [4].

The PCS is defined as

$$|\xi; k\rangle = (1 - |\xi|^2)^k \sum_{m=0}^{\infty} \sqrt{\frac{\Gamma(m+2k)}{m! \Gamma(2k)}} \xi^m |m; k\rangle, \quad (11)$$

where  $\xi = -\tanh(\frac{r}{2}) \exp(-i\Phi)$ , with  $|\xi| \in (0, 1)$ ,  $r \in (-\infty, \infty)$ ,  $\Phi \in (0, 2\pi)$ ,  $\Gamma$  stands for Gamma function and  $k$  is called Bargmann index ( $k(k-1)$  is the eigenvalue of the Casimir operator  $\hat{C} = \hat{k}_z - \frac{1}{2}(\hat{k}_+ \hat{k}_- + \hat{k}_- \hat{k}_+)$ ). For  $k = 1/4(3/4)$  the PCS is the even (odd) parity coherent state [2, 3].

The BGCS is defined as

$$|Z; k\rangle = \sqrt{\frac{|Z|^{2k-1}}{I_{2k-1}(2|Z|)}} \sum_{m=0}^{\infty} \frac{Z^m}{\sqrt{m!\Gamma(m+2k)}} |m; k\rangle, \quad (12)$$

where  $I_k(\cdot)$  is the modified Bessel function of order  $k$ ,  $Z = |Z|\exp(i\Phi)$ ,  $\Phi \in (0, 2\pi)$  and  $k$  is the Bargmann index. It is worth mentioning that these states are the eigenstate of  $\hat{k}_-$ , i.e.  $\hat{k}_-|Z; k\rangle = Z|Z; k\rangle$ .

The explicit expressions for the expectation value of the arbitrary moments  $\langle \hat{k}_-^l(0)\hat{k}_z^m(0)\hat{k}_+^n(0) \rangle$  in both the PCS and the BGCS are given in [20].

For  $t > 0$  and as the interaction is turned on the energy exchange between the interacting subsystems starts to play a role and thus the shape of the squeezed regions (in the complex plane) depends on the ratio  $(\lambda/\omega)$ . For this reason we study such evolution for the three cases, namely, weak coupling, strong coupling and resonance case according to  $(\lambda/\omega) \ll 1$ ,  $(\lambda/\omega) \gg 1$  and  $(\lambda/\omega) = 1$ , respectively.

### III. EVOLUTION OF THE SQUEEZED REGIONS OF THE PCS

The PCS is a special type of squeezed vacuum state [21] which is essentially equivalent to the two-photon coherent state [22], and it possesses most of the properties of the ordinary coherent states, such as a completeness relation and a reproducing kernel. Also the PCS can be realized in the framework of degenerate and nondegenerate parametric amplifier [23]. The required quantities for discussing the behaviour of  $F_{x,y}(\cdot)$  in (6) are given by

$$\begin{aligned} \langle (\Delta \hat{k}_x(t))^2 \rangle &= 2k \left\{ |f(t)|^2 + \frac{[S(t) - \xi^* f(t) - \xi f^*(t)]^2}{(1 - |\xi|^2)^2} + \frac{S(t)[\xi^* f(t) + \xi f^*(t) - S(t)]}{(1 - |\xi|^2)} \right\}, \\ \langle (\Delta \hat{k}_y(t))^2 \rangle &= 2k \left\{ |G(t)|^2 + \frac{[V(t) + \xi^* G(t) + \xi G^*(t)]^2}{(1 - |\xi|^2)^2} - \frac{V(t)[\xi^* G(t) + \xi G^*(t) + V(t)]}{(1 - |\xi|^2)} \right\}, \\ \langle \hat{k}_z(t) \rangle &= \frac{k}{(1 - |\xi|^2)} \left\{ (1 + |\xi|^2)R_3(t) + 2[\xi^* h(t) + \xi h^*(t)] \right\}, \end{aligned} \quad (13)$$

where

$$f(t) = \frac{1}{2}[R_1(t) - iJ(t)], \quad G(t) = \frac{1}{2}[J(t) - iR_2(t)], \quad h(t) = \frac{1}{2}[S(t) - iV(t)]. \quad (14)$$

From (13) and (6) it is evident that the fluctuations are independent of the Bargmann index  $k$ .

Initially, at  $t = 0$ , the results (13), (14) with (6) lead to the following expressions:

$$F_x(r, \Phi, t = 0) = \frac{\tanh^2(\frac{r}{2})}{1 - \tanh^4(\frac{r}{2})} [(1 + \cosh r) \cos^2 \Phi - 1], \quad (15)$$

and

$$F_y(r, \Phi, t = 0) = \frac{\tanh^2(\frac{r}{2})}{1 - \tanh^4(\frac{r}{2})} [(1 + \cosh r) \sin^2 \Phi - 1]. \quad (16)$$

The condition for squeezing the  $\hat{k}_x$ - or the  $\hat{k}_y$ -component is  $F_x < 1$  or  $F_y < 1$ , namely, the results first obtained in [21],

$$1 + \cos^2 \Phi \sinh^2(2r) \leq \cosh(2r) \quad (17)$$

or

$$1 + \sin^2 \Phi \sinh^2(2r) \leq \cosh(2r), \quad (18)$$

respectively.

It is clear from (15) and (16) that the squeezed regions are symmetric in  $r$  and periodic in  $\Phi$  with period  $\pi$ , i.e.,  $F_j(r, \Phi, t = 0) = F_j(-r, \Phi + \pi, t = 0)$ . Furthermore,  $F_x(\cdot)$  connects with  $F_y(\cdot)$  through the relation

$$F_y(r, \Phi, t = 0) = F_x(r, \Phi + \frac{\pi}{2}, t = 0) \quad (19)$$

and thus have similar behaviour with  $F_y$  shifted by  $\pi/2$  along the  $\Phi$ -axis. It is also clear from (15) that  $F_x(\cdot)$  has maximum squeezing (100%) at  $\Phi = \pi/2$  and  $3\pi/2$  regardless of the values of  $r$  and it is symmetric around these lines, i.e.,  $F_x(\cdot, \Phi = \pi/2 + \epsilon, t = 0) = F_x(\cdot, \Phi = \pi/2 - \epsilon, t = 0)$  where  $\epsilon \leq \pi/2$  [21]. Furthermore, squeezed intervals on the specific lines can be obtained by applying the squeezing conditions  $F_j \leq 0$ , e.g. setting  $r = 0$  in (15) and analyzing the squeezing inequality lead to

$$\frac{3\pi}{4} \geq \Phi \geq \frac{\pi}{4}, \quad \frac{7\pi}{4} \geq \Phi \geq \frac{5\pi}{4}. \quad (20)$$

Restricting our discussion to the first region (where both of which are similar) we see that at the borders of this region the state is minimum-uncertainty state but when  $\Phi$  "evolves" the squeezing values increase gradually showing its maximum value at  $\Phi = \pi/2$ , i.e. maximum squeezing occurs at

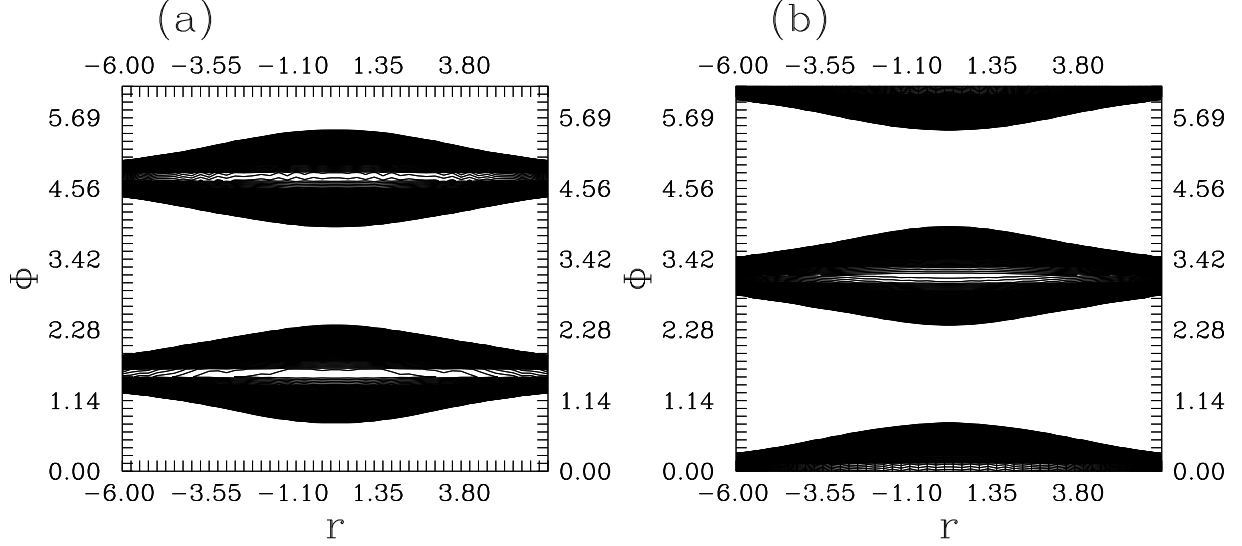


FIG. 1: The squeezing regions in the  $(r, \Phi)$ -plane of the  $\hat{k}_x$ - and  $\hat{k}_y$ -components (a) and (b), respectively, at initial time  $t = 0$ .

the most inner contours. All this information is clear in Figs. 1 where we have plotted the squeezed regions for  $F_x(\cdot)$  and  $F_y(\cdot)$  in the  $(r, \Phi)$ -plane for given values of the parameters. Comparison of Fig. 1a and 1b leads to the fact that there are specific regions in the  $(r, \Phi)$ -plane for which neither the  $\hat{k}_x$ - nor the  $\hat{k}_y$ -quadrature is squeezed. Furthermore, squeezing cannot be established in the two quadratures simultaneously.

Now for  $t > 0$  we discuss the evolution of squeezed regions of  $F_j(r, \Phi, t)$  for the system under consideration in  $(r, \Phi)$ -plane for the three cases mentioned above.

### A. weak coupling

In this case  $(\lambda/\omega) \ll 1$ , i.e. the frequency detuning parameter  $\omega$  is much greater than the coupling constant  $\lambda$ . The exact expressions for the variances in (13) can be obtained easily for the zeroth order of  $(\lambda/\omega)$ , which have similar forms as those of the initial ones (15) and (16) but with  $\Phi \rightarrow \Phi + 2\omega t$ . This means that under this condition the initial state  $|\xi, k\rangle$  evolves into the dynamical state (up to a constant phase)  $|\xi \exp(2i\omega t), k\rangle$ . More illustratively, the free part in the Hamiltonian (1) acts much effectively on the behaviour of the dynamical system than the interaction part and then the dynamical state of the system can be expressed as:

$$\hat{U}(t)|\xi, k\rangle \simeq \exp(2i\omega t \hat{k}_z)|\xi, k\rangle = |\xi \exp(2i\omega t), k\rangle. \quad (21)$$

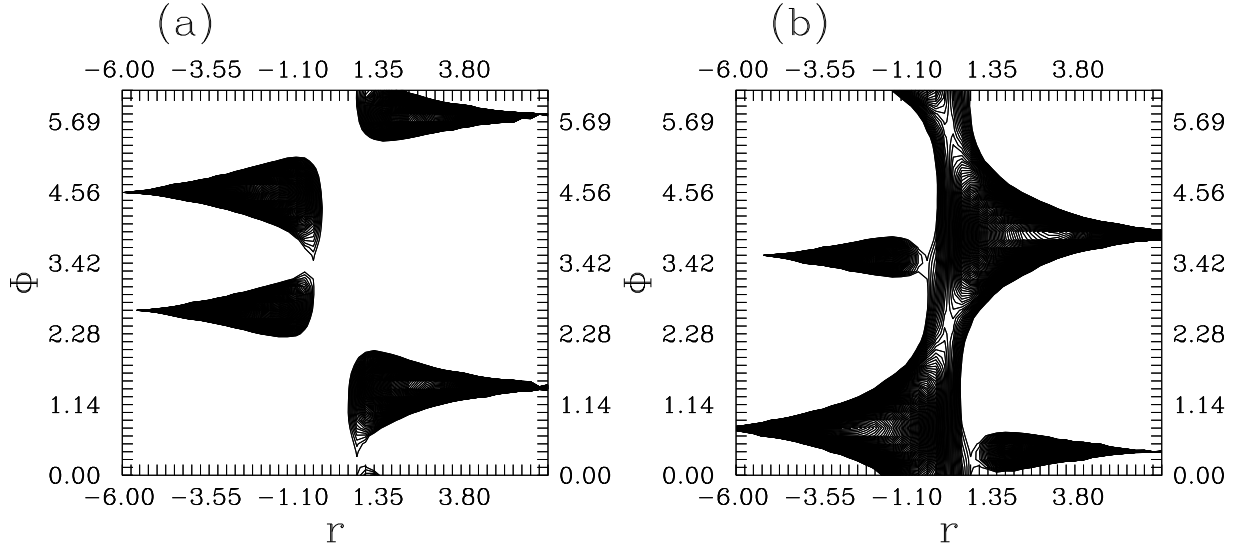


FIG. 2: The squeezing regions in the  $(r, \Phi)$ -plane of the  $\hat{k}_x$ - and  $\hat{k}_y$ -components (a) and (b), respectively, for the normalized time  $t_\lambda = t\lambda = \pi/2$  and  $\omega/\lambda = 3$

So it is obvious that in this case the initial squeezed regions move along the  $\Phi$ -axis by an amount  $2\omega t$  having typical shapes and sizes as those of the initial regions. This situation is similar to that of the  $SU(2)$  systems [16] in atomic coherent state. For completeness, we provide Figs. 2a,b and Figs. 3a,b for the squeezed regions of the exact forms (13) when  $(\omega/\lambda) = 3$  and 10, respectively. From Figs. 2 it seems that the sizes of the squeezed regions are decreased compared to those of the initial ones and also the symmetry in the  $(r, \Phi)$ -plane is smeared out. These facts are remarkable by comparing Figs. 1 and 2. On the other hand, by increasing the values of  $\omega$  compared to those of  $\lambda$  the behaviour of the system starts to going to that of the initial states (compare Figs. 1 and 3) and this agrees with the discussion given above (c.f. (21)). Furthermore, generally for the weak coupling case the initial squeezing is periodically restored and the maximum squeezing occurs at the most inner contours.

### B. Strong coupling

In this case  $(\lambda/\omega) \gg 1$ , i.e. the coupling constant  $\lambda$  is much greater than the detuning parameter  $\omega$ . In this case the Rabi frequency parameter  $g$  tends to  $i\sqrt{\lambda^2 - \omega^2}$  and consequently the trigonometric functions in the dynamical solutions (8) are converted into hyperbolic functions, which are monotonically increasing functions of  $t$  and then the initial squeezing of the PCS will vanish even for very short interaction time. For instance, for large interaction time  $t$  (taking normalized



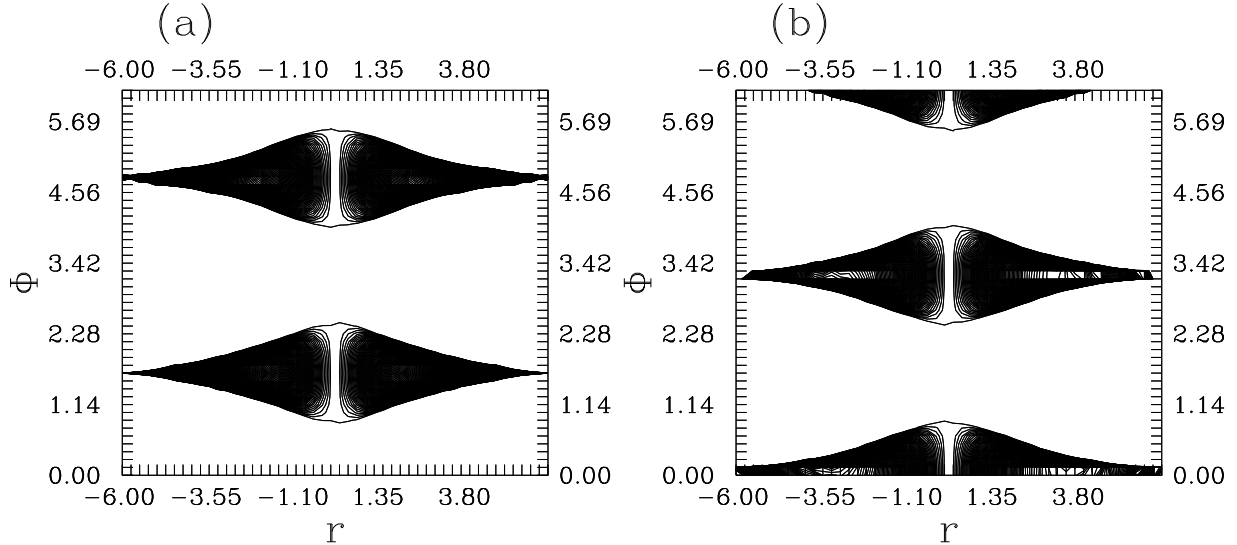


FIG. 3: The squeezing regions in the  $(r, \Phi)$ -plane of the  $\hat{k}_x$ - and  $\hat{k}_y$ -components (a) and (b), respectively, for the normalized time  $t_\lambda = t\lambda = \pi/2$  and  $\omega/\lambda = 10$

time  $\tau = gt$ ),  $\cosh(\tau) \simeq \sinh(\tau) \simeq \frac{1}{2} \exp(\tau)$  and (13) reduce to such types of proportionality

$$\langle (\Delta \hat{k}_j(t))^2 \rangle \propto \exp(4\tau), \quad j = x, y, \quad \langle \hat{k}_z(t) \rangle \propto \exp(2\tau). \quad (22)$$

This shows that the initial squeezed quadrature ( $F_j(t=0) < 0$ ) becomes unsqueezed due to the interaction with the material media regardless of the values of  $\xi$ . This situation is completely in contrast with the  $SU(2)$  case [16] where squeezing always exists and the initial squeezing values are periodically recovered. It is a feature difference between the  $SU(2)$  and  $SU(1,1)$  Lie algebraic structures. In Figs. 4a and b we have plotted the squeezed regions for the  $\hat{k}_x$ - and  $\hat{k}_y$ -components. In these figures we have considered  $\lambda$  is greater than  $\omega$  but not too much. Comparison of Figs. 1 and 4 leads to the fact that the sizes of the squeezed regions are decreased compared with those of the initial ones. Furthermore, the squeezed area regarding to the  $\hat{k}_y$ -component is decreased more rapidly than that in the  $\hat{k}_x$ -component. This is a direct consequence of the structure of the Hamiltonian (1). Also the symmetry in the  $(r, \Phi)$ -plane for the chosen values is remarkable.

### C. Resonance case

In this case  $(\lambda/\omega) = 1$ , i.e. the coupling constant  $\lambda$  is equal to the detuning parameter  $\omega$ . This manifests itself in the quadrature variances, which become polynomials of the normalized time

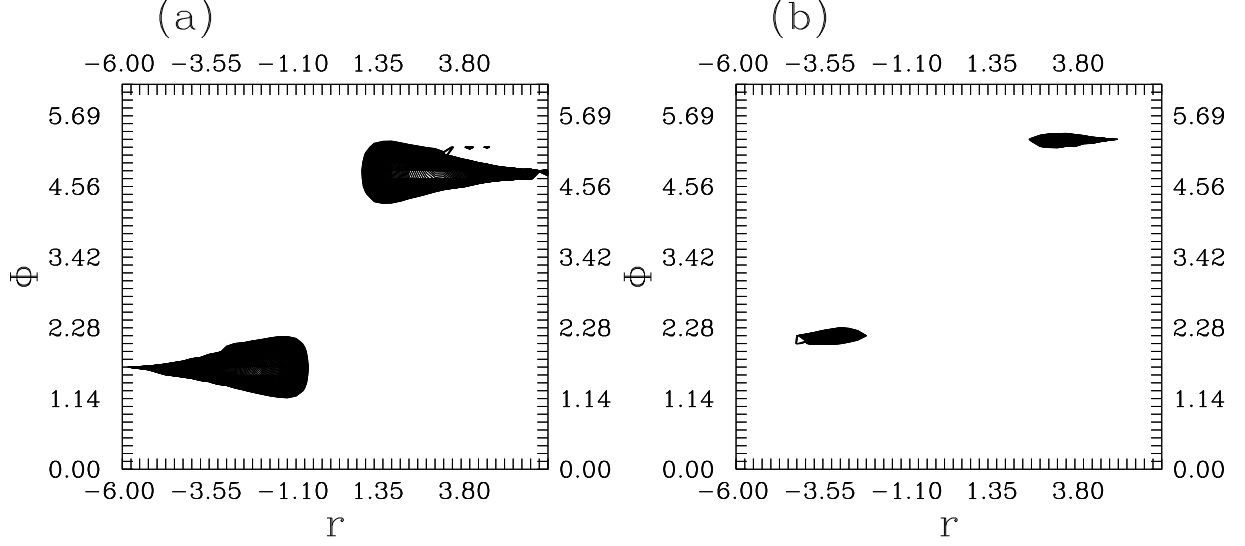


FIG. 4: The squeezed regions in the  $(r, \Phi)$ -plane of the  $\hat{k}_x$ - and  $\hat{k}_y$ -components (a) and (b), respectively, at  $t_\omega = t\omega = \pi/4$  and  $\lambda/\omega = 2$ .

$\tau = t\lambda = t\omega$ . In this case expressions (13) reduce to

$$\langle (\Delta \hat{k}_x(\tau))^2 \rangle = 2k \left\{ \tau^4 \chi^2 + \tau^2 [\chi \sinh r \cos \Phi + \sinh^2 r \sin^2 \Phi] \right. \quad (23)$$

$$\left. - 2\tau^3 \chi \sinh r \sin \Phi - \frac{\tau}{2} \sinh^2 r \sin(2\Phi) + \varepsilon(\Phi) \right\},$$

$$\langle (\Delta \hat{k}_y(\tau))^2 \rangle = 2k \left\{ \tau^2 \chi^2 - \tau \chi \sinh r \sin \Phi + \varepsilon\left(\Phi + \frac{\pi}{2}\right) \right\}, \quad (24)$$

$$\langle \hat{k}_z(\tau) \rangle = 2k \left\{ \tau^2 \chi - \tau \sinh r \sin \Phi + \frac{1}{2} \cosh r \right\}, \quad (25)$$

where

$$\chi = \cosh r - \sinh r \cos \Phi, \quad \varepsilon(\Phi) = \frac{1}{4} [1 + \sinh^2 r \cos^2 \Phi]. \quad (26)$$

It is evident that (23) is a polynomial of order four in  $\tau$ , however, (24) and (25) are polynomials of order two. This leads to (one can easily check) when  $\tau \gg 1$ ,  $F_y(\cdot)$  exhibits always squeezing, which becomes time-independent (steady-state squeezing). Nevertheless, this is not the case for  $F_x(\cdot)$  where squeezing is completely suppressed as the time evolves. For  $\tau \gg 1$  one can deduce straightforwardly that  $F_y(\cdot)$  takes the form

$$F_y(r, \Phi) = 2\chi - 1. \quad (27)$$

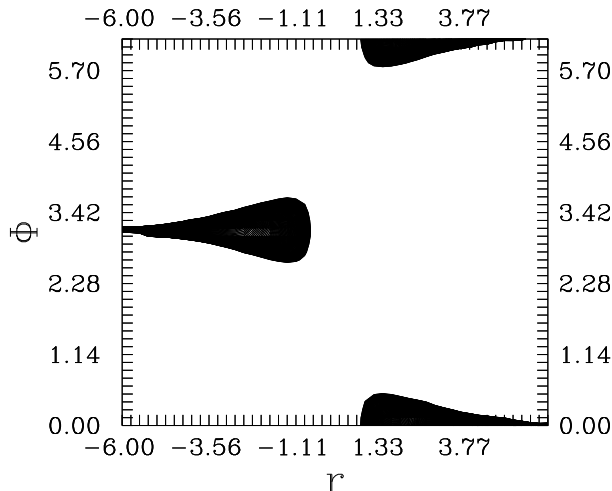


FIG. 5: The squeezed regions in the  $(r, \Phi)$ -plane of the  $\hat{k}_y$ -component for normalized time  $\tau = 3\pi$  in the resonance case.

In other words, the squeezing condition for the  $\hat{k}_y$ -component is

$$2(\cosh r - \sinh r \cos \Phi) - 1 \leq 0. \quad (28)$$

Inequality (28) fails for  $\Phi = m\pi/2$ ,  $m = 1, 3, 5, \dots$  regardless the value of  $r$  and also for  $r = 0$  regardless the value of  $\Phi$ . On the contrary, (28) is satisfied for both  $r > 0$  and  $\Phi = m\pi$ ,  $m = 0, 2, 4, \dots$  and also for  $r < 0$  and  $\Phi = m\pi$ ,  $m = 1, 3, 5, \dots$ . Inequality (28) can be solved easily to some representative lines. For example, on  $\Phi = 0$  (or  $\Phi = \pi$ ) it gives  $r \geq 0.69$ , where  $F_y(., r \simeq 0.69, .) \simeq 0$ . Furthermore, maximum value of squeezing can be obtained when  $F_y = -1$ , i.e. when  $\chi = 0$  and this leads to  $\cos \Phi = \coth r$ . That is when  $\Phi = 0$ ,  $r \rightarrow \infty$  maximum squeezing is achieved. Summing up on the line  $\Phi = 0$  the system exhibits minimum-uncertainty state at  $r \simeq 0.69$  and then the values of the squeezing gradually increase as  $r$  increases. All these analytical facts are noticeable in Fig. 5, where we have plotted  $F_y(., .)$ . On the other hand, as we have mentioned above, the initial squeezing inherited in  $F_x(., .)$  is suppressed gradually as the interaction evolves. For example, on the line  $r = 0$  squeezing exists only when  $\tau \leq 1/\sqrt{2}$  and also maximum squeezing cannot be occurred.

#### IV. EVOLUTION OF THE SQUEEZED REGIONS OF THE BGCS

In this section we investigate the evolution of the squeezed regions in the plane  $(|Z|, \Phi)$  when the system is initially in the state BGCS given by (12). It is worth mentioning that the BGCS has similar properties as the ordinary (Glauber) coherent state in the sense that it is unsqueezed state

and a minimum-uncertainty state (so-called  $SU(1,1)$  intelligent state). The required quantities appearing in the expressions of  $F_{x,y}(t)$  in (6) for the BGCS are given by

$$\begin{aligned}
\langle(\Delta\hat{k}_x(t))^2\rangle &= 2|f(t)|^2 \left[ k + \frac{|Z|I_{2k}(2|Z|)}{I_{2k-1}(2|Z|)} \right] - S(t)[Z^*f(t) + Zf^*(t)] \\
&+ |Z|S^2(t) \left[ |Z| \left( 1 - \frac{I_{2k}^2(2|Z|)}{I_{2k-1}^2(2|Z|)} \right) + (1-2k)\frac{I_{2k}(2|Z|)}{I_{2k-1}(2|Z|)} \right], \\
\langle(\Delta\hat{k}_y(t))^2\rangle &= 2|G(t)|^2 \left[ k + \frac{|Z|I_{2k}(2|Z|)}{I_{2k-1}(2|Z|)} \right] - V(t)[Z^*G(t) + ZG^*(t)] \\
&+ |Z|V^2(t) \left[ |Z| \left( 1 - \frac{I_{2k}^2(2|Z|)}{I_{2k-1}^2(2|Z|)} \right) + (1-2k)\frac{I_{2k}(2|Z|)}{I_{2k-1}(2|Z|)} \right], \\
\langle\hat{k}_z(t)\rangle &= R_3(t) \left[ k + \frac{|Z|I_{2k}(2|Z|)}{I_{2k-1}(2|Z|)} \right] + Z^*h(t) + Zh^*(t),
\end{aligned} \tag{29}$$

where  $f(t)$ ,  $G(t)$  and  $h(t)$  are given in (14). Initially ( $t = 0$ ) from (29) one recovers the no-squeezing minimum uncertainty relation  $\langle(\Delta\hat{k}_{x,y}(0))^2\rangle = \frac{1}{2}|\langle\hat{k}_z(0)\rangle|$  derived in [20]. For  $t > 0$  and throughout the discussion of the present section we emphasize on the two limiting cases, namely, the weak and strong intensity limits,  $|Z| \ll 1$  and  $|Z| \gg 1$ , respectively, provided that the interaction time and the Bargmann index  $k$  are finite. These two approaches will give a good visualization for the behaviour of the system in a whole  $(|Z|, \Phi)$ -plane. For the weak intensity case (29) can be simplified into the forms

$$\begin{aligned}
\langle(\Delta\hat{k}_x(t))^2\rangle &\simeq [2|f(t)|^2 + S^2(t)]\frac{|Z|^2}{2k} + 2k|f(t)|^2 - S(t)[Z^*f(t) + Zf^*(t)], \\
\langle(\Delta\hat{k}_y(t))^2\rangle &\simeq [2|G(t)|^2 + V^2(t)]\frac{|Z|^2}{2k} + 2k|G(t)|^2 - V(t)[Z^*G(t) + ZG^*(t)], \\
\langle\hat{k}_z(t)\rangle &\simeq R_3(t)\left(k + \frac{|Z|^2}{2k}\right) + Z^*h(t) + Zh^*(t),
\end{aligned} \tag{30}$$

while for the strong intensity case they take the forms

$$\begin{aligned}
\langle(\Delta\hat{k}_x(t))^2\rangle &\simeq 2|f(t)|^2(k + |Z|) - S(t)[Z^*f(t) + Zf^*(t)] + |Z|(1-2k)S^2(t), \\
\langle(\Delta\hat{k}_y(t))^2\rangle &\simeq 2|G(t)|^2(k + |Z|) - V(t)[Z^*G(t) + ZG^*(t)] + |Z|(1-2k)V^2(t), \\
\langle\hat{k}_z(t)\rangle &\simeq R_3(t)(k + |Z|) + Z^*h(t) + Zh^*(t).
\end{aligned} \tag{31}$$

In the following we discuss the different cases as we did in section 3.

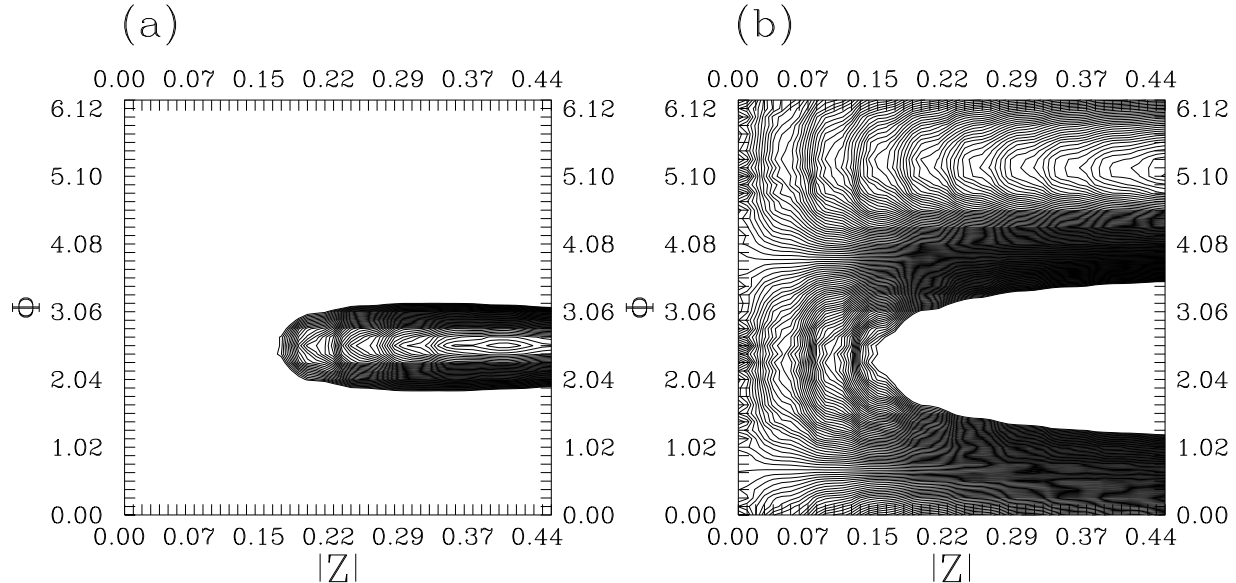


FIG. 6: The squeezed regions in the  $(|Z|, \Phi)$ -plane of the  $\hat{k}_x$ - and  $\hat{k}_y$ -components (a) and (b), respectively, for  $k = 0.5, t_\lambda = t\lambda = 1$  and  $\omega/\lambda = 3$ .

#### A. weak coupling

As we mentioned above the BGCS is not a squeezed state. So that following similar discussion as that given in subsection 3.1 one can prove that for weak coupling case the system evolves always in a minimum-uncertainty state. Now we discuss the case when  $\omega$  is greater than  $\lambda$  but not too much. In this case we have noted that squeezing can be occurred. This of course arises from the interaction of the field with the nonlinear medium. This situation can be recognized analytically when  $|Z| \rightarrow 0$ , the quantities  $F_j(\cdot)$  reduce to

$$F_x(\tau) = \frac{2\lambda^2}{g^2 R_3(\tau)} \left[ \frac{2\omega^2}{g^2} \sin^2(\tau) - 1 \right] \sin^2(\tau), \quad (32)$$

$$F_y(\tau) = \frac{2\lambda^2}{g^2 R_3(\tau)} \cos(2\tau) \sin^2(\tau),$$

where  $\tau = gt$ . We have to stress that  $R_3(t)$  is always positive (c.f. (8)). From (32) squeezing can occur in  $F_x$  or  $F_y$ , at particular values of the interaction parameters, e.g. maximum squeezing can be generated in  $F_y$  at  $\tau = \pi/2$ . Also when  $(\lambda/\omega) \ll 1$ , (32) give  $F_{x,y} \simeq 0$ , which agree with the above conclusion. Information about the weak intensity case is shown in Figs. 6 for given values of the system parameters. Maximum squeezing in the  $\hat{k}_x$ -component occurs at the most inner contour, however, for the  $\hat{k}_y$ -component it occurs around the line  $\Phi \simeq 7\pi/4$ . Also there is a lack of symmetry in the phase plane somewhat similar to the PCS case. Generally, squeezing is sensitive to the values of Bargmann index  $k$ , in contrast with the PCS case, which decreases as

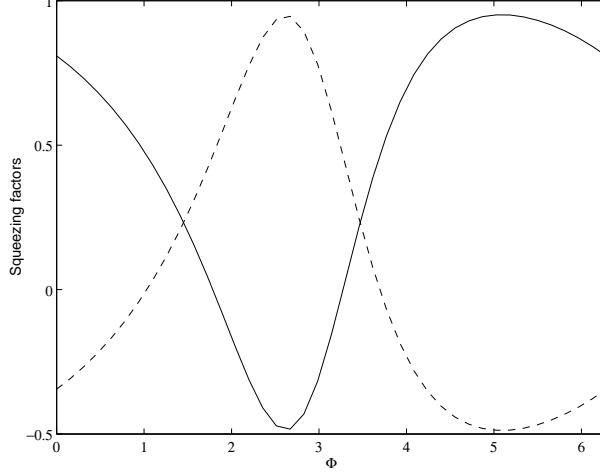


FIG. 7: Squeezing factors  $F_j(\cdot)$  against  $\Phi$ -axis the  $\hat{k}_x$ - and  $\hat{k}_y$ -components corresponding to solid and dashed curves, respectively, for  $|Z| = 200, k = 0.5, t_\lambda = t\lambda = \pi/2$  and  $\omega/\lambda = 3$ .

$k$  increases. On the other hand, for strong intensity case and for finite values of  $k$ ,  $F_j(\cdot)$  become  $|Z|$ -independent. This is obvious from (31) where all quantities are polynomials of first order in  $|Z|$ . For this reason we study squeezing occurrence regarding to  $\Phi$  for fixed values of  $|Z|$ . This is given in Fig. 7 for the shown values of the parameters. From this figure one observes that the maximum value of squeezing is 50%. From figures 6 and 7 we see that the squeezed area of  $F_x(F_y)$  decreases (increases) as  $|Z|$  gets larger and then it persists.

### B. Strong coupling

In this case  $\lambda \gg \omega$  and the system has a time-dependent amplifying nature, which decreases the amount of squeezing (as we have seen in the PCS case). Nevertheless, under certain conditions, squeezing can be detected in the system. This can be seen analytically in the limiting case  $|Z| \rightarrow 0$ , where  $F_j(\cdot)$  read

$$F_x(\tau) = \frac{2\lambda^2}{g^2 R_3(\tau)} \left[ \frac{2\omega^2}{g^2} \sinh^2(\tau) - 1 \right] \sinh^2(\tau), \quad (33)$$

$$F_y(\tau) = \frac{2\lambda^2}{g^2 R_3(\tau)} \cosh(2\tau) \sinh^2(\tau),$$

where  $\tau = gt$ . From (33) it is clear that squeezing occurs only in the  $\hat{k}_x$ -component, in particular, when the interaction time is small, specifically, for times such that,

$$\sinh(\tau) \leq \frac{g}{\sqrt{2\omega}}. \quad (34)$$

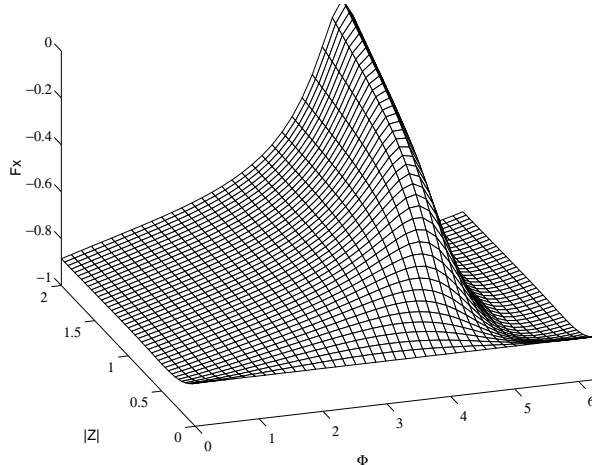


FIG. 8: Squeezing factor  $F_x(\cdot)$  for  $k = 0.5$ ,  $t_\omega = t\omega = \pi/20$  and  $\lambda/\omega = 10$ .

In Fig. 8 we have plotted  $F_x(\cdot)$  for given values of the interaction parameters. Fig. 8 exhibits single-peak structure. More illustratively, maximum value of squeezing occurs for  $\Phi = 0, 2\pi$ , however, on the line  $\Phi = \frac{3}{2}\pi$  squeezing values decrease monotonically as  $|Z|$  increases, eventually suppressed and hence  $F_x(\cdot)$  becomes  $|Z|$ -independent. Further, squeezing values are sensitive to the Bargmann index  $k$ , in particular, for finite  $|Z|$ . For instance, as  $k$  increases the squeezed region in  $(|Z|, \Phi)$ -plane increases, too.

### C. Resonance case

As in section 3, at resonance ( $\lambda = \omega$ ) the variances and the expectation values are polynomials in the normalized time  $\tau = t\lambda = t\omega$ . In the very weak intensity limit,  $|Z| \rightarrow 0$ , one obtains

$$F_x(\tau) = \frac{2\tau^2(2\tau^2 - 1)}{(2\tau^2 + 1)}, \quad F_y(\tau) = \frac{\tau^2}{(2\tau^2 + 1)}, \quad (35)$$

which shows that  $F_x(\cdot)$  exhibits squeezing for  $\tau \leq 1/\sqrt{2}$ . On the other hand, numerical investigation shows that with the system initially ( $\tau = 0$ ) in a non-squeezed minimum-uncertainty state and as the interaction is switched on squeezing is generated for a short interaction time in both quadratures components  $\hat{k}_x, \hat{k}_y$  for weak intensity (, i.e.  $|Z| < 1$ ) (see Figs. 9) and eventually suppressed as the interaction time evolves. Notice that the behaviour of  $F_x(\cdot)$  and  $F_y(\cdot)$  in the present resonance case is the corresponding reverse behaviour in the weak coupling case ( $\omega \gg \lambda$ ) of Fig. 6. Similar behaviour has been noted for large values of  $|Z|$  (see Fig. 7).

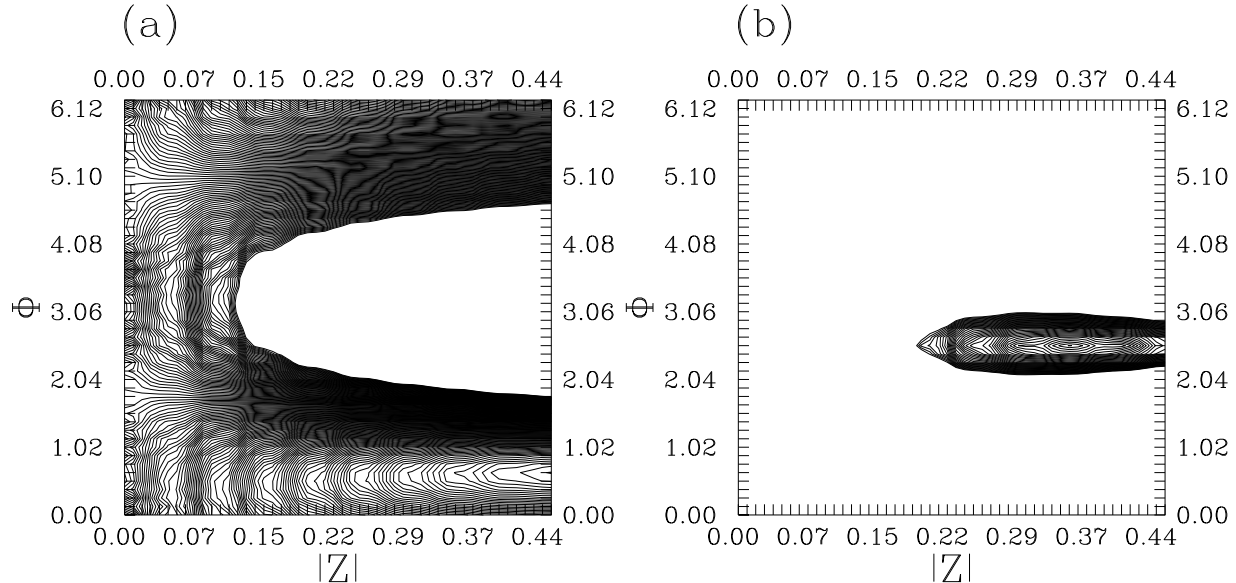


FIG. 9: The squeezed regions in the  $(|Z|, \Phi)$ -plane of the  $\hat{k}_x$ - and  $\hat{k}_y$ -components (a) and (b), respectively, for  $k = 0.5$  and  $\tau = \pi/6$ .

## V. SUMMARY OF THE RESULTS

Throughout this paper we have analysed the evolution of the squeezed regions for the dynamical system whose Hamiltonian is a linear combination of the  $SU(1, 1)$  Lie algebra generators. We have considered two initial states, namely, the PCS and the BGCS. We have investigated the three cases: weak coupling  $(\omega/\lambda) \gg 1$ , strong coupling  $(\omega/\lambda) \ll 1$  and resonance case  $(\omega/\lambda) = 1$ .

For the PCS when  $t = 0$  the squeezed regions in the  $(r, \Phi)$ -plane are symmetric around specific lines on the  $\Phi$ -axis and there is a direct relation between  $F_x$  and  $F_y$ . Also maximum squeezing occurs at the most inner contours. However, when the interaction is switched on the features of the initial squeezed regions are changed and the following results have been obtained:

- (i) For weak coupling and when  $\omega$  is much greater than  $\lambda$  the initial squeezed regions move along the  $\Phi$ -axis by an amount  $2\omega t$ . Nevertheless, when  $\omega$  is greater than  $\lambda$  but not too much the size of the squeezed regions are decreased compared to those of the initial ones.
- (ii) For strong coupling  $\lambda \gg \omega$  the initial inherited squeezed regions for the system are lost, whereas when  $\lambda$  is greater than  $\omega$  but not too much the area of the squeezed regions are decreased compared to those of the initial ones. Further, the squeezed region associated with  $F_y$  is decreased faster than that with  $F_x$ .
- (iii) For the resonance case  $\omega = \lambda$ , the variances associated with the  $\hat{k}_x$ - and  $\hat{k}_y$ -components become polynomials of the normalized time. In this case  $F_y$  exhibits steady-state squeezing, whereas the



initial squeezing inherited in  $F_x$  is completely suppressed as the time evolves.

On the other hand, the BGCS is a minimum-uncertainty state, however, as result of the interaction with the nonlinear medium squeezing can be generated. The results related to this case has been restricted to two limiting cases, namely, weak intensity case  $|Z| \ll 1$  and strong intensity case  $|Z| \gg 1$ , and can be summarized as follows:

- (i) For both weak coupling and weak intensity maximum squeezing in the  $(|Z|, \Phi)$ -plane occurs in the  $F_x$  and  $F_y$  at the most inner contours and on the line  $\Phi = 7\pi/4$ , respectively. However, in the strong intensity regime  $F_j, j = x, y$  become  $|Z|$ -independent and the squeezed area for  $F_x(F_y)$  decreases (increases) as  $|Z|$  increases.
- (ii) For strong coupling squeezing occurs for short time interaction only in the  $F_x$ , which exhibits single-peak structure in the  $(|Z|, \Phi)$ -plane. Maximum value of squeezing occurs at  $\Phi = 0, 2\pi$  and as  $|Z|$  increases  $F_x$  gradually becomes  $|Z|$ -independent.
- (iii) For the resonance case the variances associated with the  $\hat{k}_x$ - and  $\hat{k}_y$ -components become polynomials of the normalized time, as in the PCS case. For this case squeezing have been detected for short interaction time in both quadratures and the behaviour of the  $F_x(F_y)$  is almost as that of  $F_y(F_x)$  for the weak coupling case.

## References

- 
- [1] Perelomov A M 1972 *Commun. Math. Phys.* **26** 222; Perelomov A M 1986 *Generalized coherent states and their applications* (Berlin: Springer).
  - [2] Dodonov V V, Malkin I A and Mank'o V I 1974 *Physica* **72** 597.
  - [3] Hillery M 1987 *Phys. Rev. A* **36** 3796; Bužek V, Vidiella-Barranco A and Knight P L 1992 *Phys. Rev. A* **45** 6570; El-Orany F A A 2002 *Phys. Rev. A* **65** 043814.
  - [4] Barut A O and Girardello L 1971 *Commun. Math. Phys.* **21** 41.
  - [5] Horn D and Silver R 1971 *Ann. of Phys.* **66** 509.
  - [6] Bhaumik D, Bhaumik K and Dutt-Roy B 1976 *J. Phys. A* **9** 1507.
  - [7] Skagerstam B S 1979 *Phys. Rev. D* **19** 2471.
  - [8] Agarwal G S 1988 *J. Opt. Soc. Am. B* **5** 1940.
  - [9] Celeghini E, Rasetti M, Tarlini M and Vitiello G 1989 *Mod. Phys. Lett.* **3** 1213; Celeghini E, Rasetti M and Vitiello G 1992 *Ann. of Phys.* **215** 156; Gerry C C, Ma P K and Vrscaj E R 1989 *Phys. Rev. A* **39** 668; Ban M 1992 *J. Math. Phys.* **33** 3213.

- [10] Yurke B, McCall S L and Klauder J R 1986 *Phys. Rev. A* **33** 4033.
- [11] Brif C and Ben-Aryeh Y 1996 *Quant. Semiclass. Opt.* **8** L1.
- [12] Brif C and Mann A 1997 *Quant. Semiclass. Opt.* **9** 889.
- [13] Gerry C C, Gou S C and Steinbach J 1997 *Phys. Rev. A* **55** 630.
- [14] Wineland D J, Bollinger J J, Itano W M, More F L and Heinzen D J 1992 *Phys. Rev. A* **46** 6797; Wineland D J, Bollinger J J, Itano W M and Heinzen D J 1994 *Phys. Rev. A* **50** 67; Agarwal G S and Puri R R 1994 *Phys. Rev. A* **49** 496.
- [15] Caves C M 1981 *Phys. Rev. D* **23** 1693; Bondurant R S and Shapiro J H 1984 *Phys. Rev. D* **30** 2584; Peřinová V, Lukš A and Křepelka J 2000 *J. Opt. B: Quant. Semiclass. Opt.* **2** 81.
- [16] Hassan S S, Abdalla MS, Abd Al-Kader G M and Hanna L A-M 2002 *J. Opt. B: Quant. Semiclass. Opt.* **4** S204.
- [17] Bužek V 1990 *J. Mod. Opt.* **37** 303.
- [18] Walls D F and Milburn G J 1994 *Quantum Optics* (Berlin: Springer); Aravind P K 1988 *J. Opt. Soc. Am. B* **5** 1545.
- [19] Abdalla M S, El-Orany F A A and Peřina J 2000 *Act. Phys. Slovaca* **50** 613.
- [20] Ban M 1993 *J. Opt. Soc. Am. B* **10** 1347.
- [21] Wódkiewicz K and Eberly J H 1985 *J. Opt. Soc. Am. B* **2** 458.
- [22] Yuen H P 1976 *Phys. Rev. A* **13** 2226.
- [23] Gerry C C 1991 *J. Opt. Soc. Am. B* **8** 685.